January 2015

APPLICATION OF BIODYNAMIC IMAGING FOR PERSONALIZED CHEMOTHERAPY IN CANINE LYMPHOMA

Michelle Renee Custead
Purdue University

Graduate School Form 30
Updated 1/15/2015

PURDUE UNIVERSITY
GRADUATE SCHOOL
Thesis/Dissertation Acceptance

This is to certify that the thesis/dissertation prepared

By Michelle R. Custead

Entitled
APPLICATION OF BIODYNAMIC IMAGING FOR PERSONALIZED CHEMOTHERAPY IN CANINE LYMPHOMA

For the degree of Master of Science

Is approved by the final examining committee:

Michael O. Childress Chair	Deborah W. Knapp
Deepika Dhawan	

To the best of my knowledge and as understood by the student in the Thesis/Dissertation Agreement, Publication Delay, and Certification Disclaimer (Graduate School Form 32), this thesis/dissertation adheres to the provisions of Purdue University's "Policy of Integrity in Research" and the use of copyright material.

Approved by Major Professor(s): Michael O. Childress

Approved by: J. C. Scott-Moncrieff 6/24/2015

Head of the Departmental Graduate Program Date

APPLICATION OF BIODYNAMIC IMAGING FOR PERSONALIZED CHEMOTHERAPY IN CANINE LYMPHOMA

A Thesis

Submitted to the Faculty

of

Purdue University

by

Michelle R Custead

In Partial Fulfillment of the

Requirements for the Degree

of

Master of Science

August 2015

Purdue University

West Lafayette, Indiana

For my family

ACKNOWLEDGEMENTS

Dr. Nolte, Dr. Ran and Dr. Turek provided valuable contributions including assistance to the conception of biodynamic imaging, the generation of the data pertaining to biodynamic imaging, data analysis and study design.

The sincerity and generosity of Michael Childress' mentorship throughout this project immensely strengthened its final form and to him I am incredibly thankful.

The work presented in this Master's Thesis was supported by an ACORN grant (No. 02092-A) from The American Kennel Club, Canine Health Foundation and a Purdue Department of Veterinary Clinical Sciences Graduate Student Competitive Research Award.

TABLE OF CONTENTS

Page

LIST OF TABLES vi

LIST OF FIGURES vii

LIST OF ABBREVIATIONS viii

ABSTRACT ix

CHAPTER 1. INTRODUCTION 1

1.1 Background on Lymphoma 1

CHAPTER 2. LITERATURE REVIEW 4

2.1 Introduction to Personalized Medicine 4

2.2 Introduction to Biodynamic Imaging (BDI) 6

2.3 Preliminary BDI Data 12

2.4 Use of Dogs as a Model for Human Non-Hodgkin's Lymphoma 15

CHAPTER 3. APPLICATION OF BIODYNAMIC IMAGING FOR PERSONALIZED CHEMOTHERAPY IN CANINE LYMPHOMA 17

3.1 Statement of Purpose 17

3.2 Materials and Methods 18

3.2.1 Study Animals 18

3.2.2 Clinical Staging and Treatment of Study Animals 19

3.2.3 Assessment of Clinical Endpoints 20

3.2.4 Biodynamic Imaging 21

3.2.5 Statistical Analysis 24

3.3 Results 27

CHAPTER 4. CONCLUSION 37

WORKS CITED 43

Page

VITA 47
PUBLICATION 50

LIST OF TABLES

Table Page

Table 1 Dynamic motility biomarkers for responsive and non-responsive dogs..... 25

Table 2 Clinical variables for 10 treated dogs. 28

LIST OF FIGURES

Figure Page

Figure 1 Motility contrast images comparing tumor spheroids of differing inherent motility 8

Figure 2 Change in cellular motion following ex vivo drug therapy in tumor spheroids of differing drug sensitivity 9

Figure 3 Example of drug response spectrogram 11

Figure 4 Preliminary motility contrast images of 2 dogs with differing responses. 13

Figure 5 Preliminary drug response spectrograms of 2 dogs with differing responses. ... 14

Figure 6 Schematic diagram of the BDI instrument.. 22

Figure 7 Kaplan-Meier plot comparing sensitive vs insenstive dogs to chemotherapy. .. 29

Figure 8 Characteristic motility contrast images from the pilot study..... 31

Figure 9 Graph depicting ΔNSD as a function of time..... 32

Figure 10 All drug response spectrograms and averaged spectrogram from dog 9..... 33

Figure 11 Characteristic averaged drug response spectrograms of responders and nonresponders 34

Figure 12 Statistical relationship between BDI and outcome..... 36

LIST OF ABBREVIATIONS

BDI	Biodynamic imaging
NHL	Non-Hodgkin's lymphoma
DLBCL	Diffuse large B-cell lymphoma
PTCL-NOS	Peripheral T-cell lymphoma, not otherwise specified
OR	Objective response
PFST	Progression-free survival time
PCM	Personalized cancer medicine
NSD	Baseline normalized standard deviation
CR	Complete remission
PR	Partial remission
SD	Stable disease
PD	Progressive disease
ΔNSD	Change in NSD from baseline
BLUTAIL	Blue tail
MEM	Mid-frequency assessment
APOP	Non-linear frequency assessment
ALLF	All frequencies

ABSTRACT

Custead, Michelle R. M.S., Purdue University, August 2015. Application of Biodynamic Imaging for Personalized Chemotherapy in Canine Lymphoma. Major Professor: Michael Childress.

Biodynamic imaging (BDI) is a novel phenotypic cancer profiling technology which characterizes changes in cellular and subcellular motion in living tumor tissue samples following in vitro or ex vivo treatment with chemotherapeutics. The ability of BDI to predict clinical response to single-agent doxorubicin chemotherapy was tested in ten dogs with naturally-occurring non-Hodgkin's lymphomas (NHL). Pre-treatment tumor biopsy samples were obtained from all dogs and treated with doxorubicin (10 μM) ex vivo. BDI captured cellular and subcellular motility measures on all biopsy samples at baseline and at regular intervals for 9 hours following drug application. All dogs subsequently received treatment with a standard single-agent doxorubicin protocol. Objective response (OR) to doxorubicin and progression-free survival time (PFST) following chemotherapy were recorded for all dogs. The dynamic biomarkers measured by BDI were entered into a multivariate logistic model to determine the extent to which BDI predicted OR and PFST following doxorubicin therapy. The model showed that the sensitivity, specificity, and accuracy of BDI for predicting treatment outcome were 95%, 91%, and 93%, respectively. To account for possible over-fitting of data to the predictive model, cross-validation with a one-left-out analysis was performed, and the adjusted sensitivity,

specificity, and accuracy following this analysis were 93%, 87%, and 91%, respectively. These findings suggest that BDI can predict, with high accuracy, treatment outcome following single-agent doxorubicin chemotherapy in a relevant spontaneous canine cancer model, and is a promising novel technology for advancing personalized cancer medicine.

CHAPTER 1. INTRODUCTION

1.1 Background on Lymphoma

Multicentric lymphoma is among the most commonly diagnosed cancers in dogs[1,2]. Lymphoma, a cancer derived from lymphocytes, is sub-divided into a number of distinct clinical entities, with diffuse large B-cell lymphoma (DLBCL) being the most commonly diagnosed lymphoma in dogs and humans. Lymphoma most often presents with generalized peripheral lymphadenopathy. This presentation of the disease is referred to as multicentric and, in people, is a type of non-Hodgkin lymphoma. Another common subtype of multicentric lymphoma in dogs is peripheral T-cell lymphoma, not otherwise specified (PTCL-NOS). This subtype is much more rarely encountered in humans.

Multicentric lymphoma, because it is a cancer of the immune system, can develop anywhere but most often develops within lymphoid organs, including lymph nodes, spleen and liver. The cancer stage, which describes how many organs the cancer involves and has prognostic importance, is similar between both humans and dogs. In dogs, stage 5 represents the most clinically advanced form and includes cancer located within the bone marrow and/or within non-lymphoid organs. In stage 1, which is rarely documented in the dog, the cancer is located within only one lymph node.

Lymphoma is considered very responsive to chemotherapy and radiation therapy. However, for the vast majority of patients, localized treatments with radiation or surgery are not recommended as front-line treatment as the cancer is typically disseminated throughout the body. Radiation and surgery are useful for cancers where the disease is restricted in location. Therefore, chemotherapy is considered the treatment of choice as front-line therapy. Chemotherapy protocols incorporating doxorubicin are considered the standard of care for both dogs and humans. The protocol in humans, as compared to dogs, is often more intense, with all of the drugs being given on the same day and at higher doses. For dogs, because the goal is to extend survival while providing a good quality of life with minimal side effects, the drugs are separated, given weekly, and the doses are lowered.

Doxorubicin-based chemotherapy is the treatment of choice for this cancer. It leads to affords high initial remission rates and extension of survival for affected dogs and high cure rates for people[3-7]. However, the length of cancer remission and survival vary tremendously among individuals, with some dogs' and peoples' cancers not responding to chemotherapy at all. In addition, chemotherapy is costly, and may cause serious side effects. Therefore, only patients where a true need exists should receive therapy and, optimally, patients should be treated with drugs that are likely to work against their cancer.

A method for predicting the responsiveness of each individual's cancer to chemotherapy would be advantageous for identifying the patient that are most likely to experience benefit from chemotherapy. Conversely, specifically for pet dogs and elderly or seriously ill human patients, such a method would ideally identify those that are

unlikely to benefit from standard chemotherapy, and could then guide informed choices to not pursue a course of expensive and potentially harmful treatment. Furthermore, potentially knowing which chemotherapeutics are most likely to work against an individual's cancer could lead to personalizing their protocol with the hope of extending survival in dogs or improving cure rates for people. Due to veterinarians' focus on maintaining a good quality of life, dogs with lymphoma are rarely cured of their cancer. Because a large percentage of patients already benefit from standard of care, the greatest benefit may most likely be seen in that hidden sub-population that will not respond to front-line, standard of care therapy. Being able to detect this subpopulation with high accuracy and then knowing from which drugs they would most benefit would be extremely useful. Unfortunately, there are currently no available assays which accurately predict the responsiveness of individuals' cancers to chemotherapy and direct personalization of their treatment protocol. The purpose of this research was therefore to determine the accuracy of a novel personalized medicine technology called biodynamic imaging (BDI) for predicting response to therapy in dogs with chemotherapy-treated NHL, with the expectation that the results would have translational relevance to other canine and human cancers.

CHAPTER 2. LITERATURE REVIEW

2.1 Introduction to Personalized Medicine

The application of diagnostic tests for predicting the responsiveness of individual patients' cancers to chemotherapy is an import part of personalized cancer medicine (PCM)[8]. The goals of PCM in clinical oncology are to improve therapeutic response to chemotherapy by selecting drugs most likely to be active against an individual patient's tumor, while at the same time decreasing health care costs and treatment-associated morbidity by avoiding the use of drugs that are unlikely to be effective. Personalized cancer medicine has historically been based on the genomic and molecular profile of an individual patient's tumor[9]. For example, recently publicized disease "signatures" in human lymphoma, which segregate patients into prognostically favorable and unfavorable subsets, have been revealed utilizing gene microarrays and immunohistochemical algorithms[10-12]. While this approach has yielded some remarkable successes, several challenges still limit the routine use of personalized medicine in the cancer clinic. For example, cancer genomes are highly complex and chaotic, and genotypic aberrations may not completely predict response to drug therapy or other phenotypic tumor behaviors[13]. Additionally, genomic approaches may not adequately model the communication existing between cancer cells themselves or between cancer

cells and stromal cells within the tumor microenvironment, and such cell-cell interactions are known to exert a powerful influence upon drug response[14]. A PCM assay which characterizes the phenotypic response of cancer to drug therapy a priori, and which recapitulates cell-cell communications within the tumor at a three-dimensional tissue level, would be highly desirable for overcoming these limitations. New strategies to predict drug response are therefore crucially needed to advance the personalization of cancer chemotherapy.

2.2 Introduction to Biodynamic Imaging (BDI)

An innovative technology, called biodynamic imaging (BDI), has promise in predicting the responsiveness of an individual's cancer to certain chemotherapeutics, thus being useful as a personalized cancer medicine assay. BDI is a three-dimensional in vitro and ex vivo tissue imaging assay which uses laser-ranging and coherence-domain detection with digital holography to analyze living tissue for temporal fluctuations of intracellular motions. Otherwise stated, it is an imaging approach that measures cellular and subcellular motion, with sensitivity to detect displacements at the sub-micron level[15]. Membrane and organelle motion are inherent properties of all living cells, and there are patterns of cellular and subcellular motion that are unique to specific cellular processes, such as mitosis or apoptosis. These motion patterns are profoundly disturbed following the application of cytotoxic agents, such as cancer chemotherapy drugs, to living cells[15-19]. The ability of BDI to capture cellular motion as a metric enables direct visualization of the effect of chemotherapeutics on living, three-dimensional tumor tissue, allowing rapid, real-time temporal measurements (2 – 9+ hours) of cellular and tissue response to drugs to be made. The rapid turn-around time for this assay is optimal for enabling clinicians to make personalized, time-sensitive treatment decisions for their patients. BDI has been previously applied to the study of cellular drug responses in cultured three-dimensional tumor spheroids and ex vivo biopsy samples from murine tumor xenografts[15,17,19,20]. An et al. demonstrated that BDI can be used to differentiate tumor

spheroids derived from four different cell lines based upon their motility properties alone[19]. As illustrated in Figure 1, the four distinct tumor spheroids were derived from UMR-106 rat osteogenic sarcoma cells, HT-29 human colon carcinoma cells, DLD-1 human colon carcinoma cells, and PaCa2 human pancreatic cancer cells. When imaged with BDI, these tumor spheroids show clear differences in intracellular motion. Importantly, BDI data acquired from these tumor spheroids corresponded to the proliferative capacity of the cells from which the spheroids were derived; the cell lines with the greatest intracellular motility (PaCa2 and DLD-1) proliferate more rapidly in vitro than the cell lines showing lesser intracellular motion (UMR-106 and HT-29).

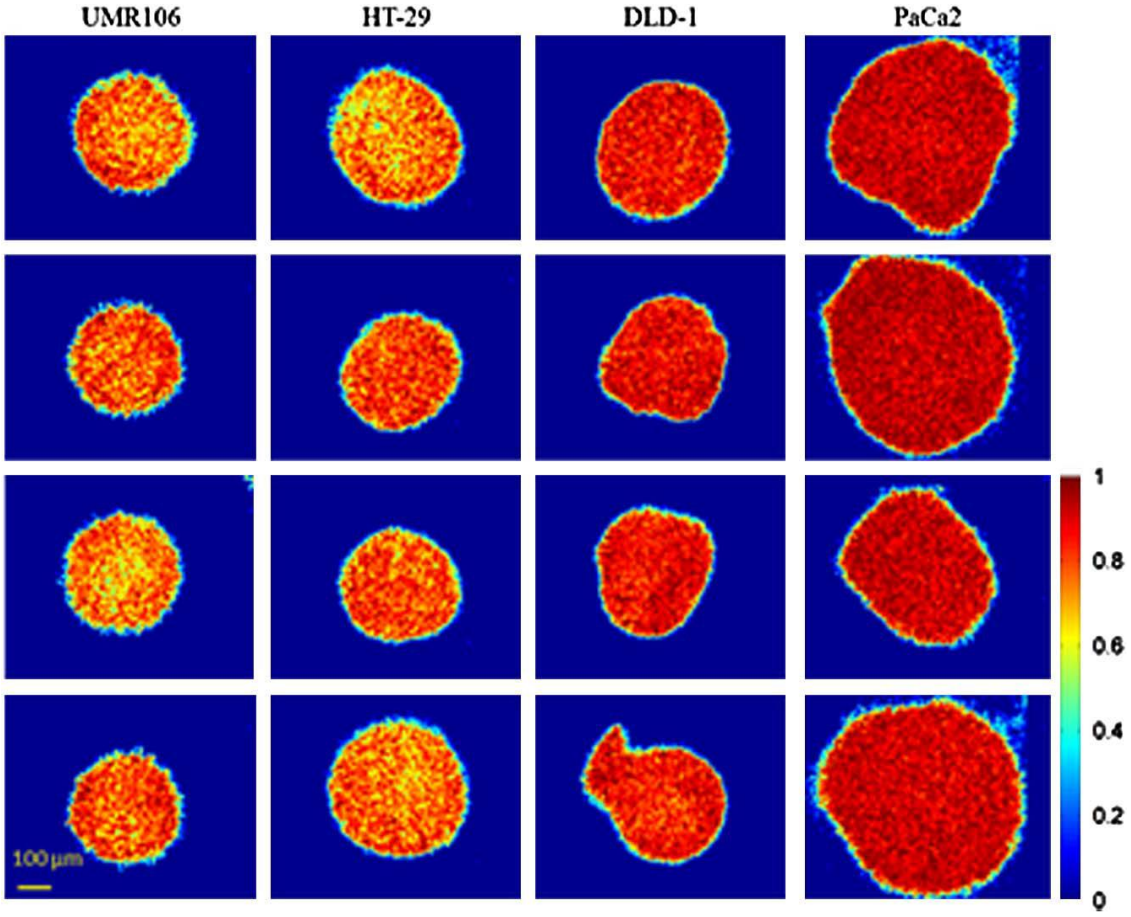

Figure 1 Motility contrast images of multicellular tumor spheroids derived from four cancer cell lines. To the right is a false color scale which describes a motility metric (normalized standard deviation, or NSD) generated from BDI data. Red pixels correspond to areas of lesser intracellular motility (and higher NSD values) and blue pixels correspond to areas of lesser intracellular motility (and lower NSD values). Note that the tumor spheroids derived from the rapidly proliferating DLD-1 and PaCa2 cell lines have greater average NSD values than spheroids derived from UMR-106 and HT-29 cells, which proliferate more slowly. (From: An R, et al. Appl Opt 2013;52:A300-9.)

An et al. further demonstrated that BDI could be used to assess the effects of cytotoxic drugs upon cancer cells[17]. In this experiment, tumor xenografts derived from two ovarian cancer cell lines were harvested from nude mice and analyzed ex vivo using BDI. The two cell lines used were: (1) A2780, which is sensitive to platinum-based

chemotherapy, and (2) A2780-CP70, which is resistant to platinum-based chemotherapy. When xenografts derived from the two cell lines were exposed to cisplatin ex vivo, BDI showed a dramatic difference in the reduction in intracellular motion observed in the platinum-sensitive cells relative to the platinum-resistant cells (Figure 2).

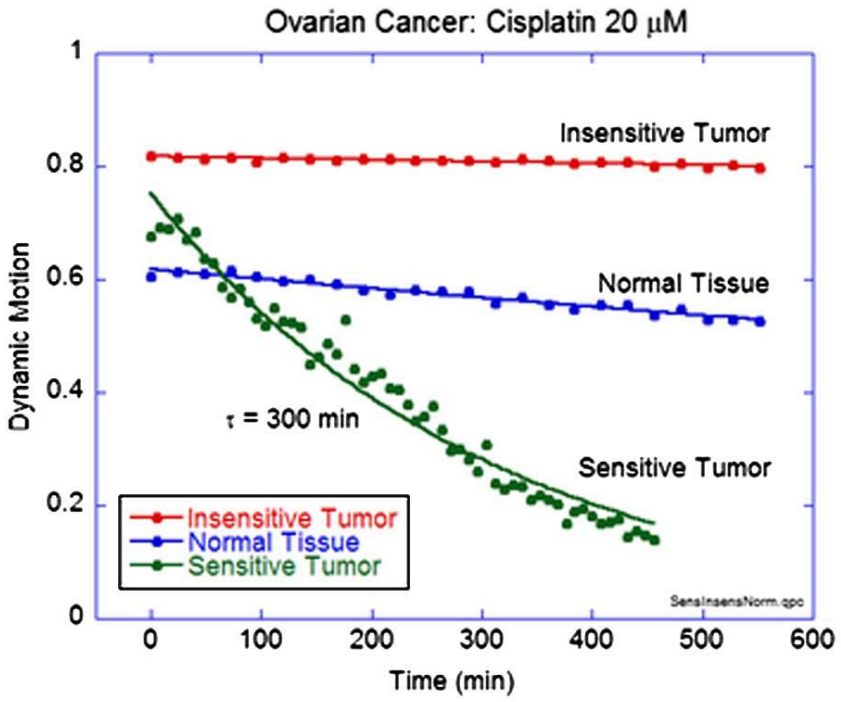

Figure 2 Graph depicting change in intracellular motility, measured using BDI, in ovarian cancer xenografts following application of cisplatin ex vivo. The x-axis represents recorded NSD values ("Dynamic Motion") and the y-axis represents time following application of cisplatin at time = 0. The red line shows change in NSD value over time in xenografts derived from the platinum-resistant cell line A2780-CP70, and the green line that for xenografts derived from the platinum-sensitive cell line A2780. Normal mouse tissue (which was physically adjacent to the tumor tissue when the xenografts were harvested) was used as a control. As expected, there was a dramatic reduction in intracellular motility in the platinum-sensitive tumor, suggesting widespread tumor cell death following cisplatin application, with little apparent decrease in motility in the platinum-resistant tumor. (From: An R, et al. Appl Opt 2013;52:A300-9.)

In addition to measuring general cell motion as a whole within tissues, biodynamic imaging has also been used to characterize more discrete features of dynamic intracellular motion within tumor cells following exposure to cytotoxic agents. Dynamic motion within a cell is attributable to morphological fluctuations in the cell membrane (e.g. ruffling, blebbing, vesicle formation), cytoplasmic streaming, and cytoskeletal reorganization, among other processes. Each of these types of motion is detected by BDI as a specific frequency – for instance, large-scale motion, such as membrane blebbing which occurs during apoptosis, corresponds to low frequencies, while small-scale motion, such as that associated with internal organelle motility, corresponds to high frequencies[17]. Following application of a cytotoxic agent to cells, BDI analyzes temporal fluctuations in intracellular motions occurring at these various frequencies, and thereby generates a spectrogram which corresponds to a "fingerprint" describing a drug's mechanism of action. An example of a drug response spectrogram generated using BDI is depicted in Figure 3. Nolte, et al. demonstrated that different drugs generate specific drug response spectrograms when applied to tumor spheroids derived from UMR-106 rat osteogenic sarcoma cells[17]. These spectrograms are unique descriptors of a particular drug's effects on a tumor. Furthermore, tissues that respond (i.e. cell death or apoptosis) will have a unique spectrogram while a different and unique spectrogram showing little to no change in motility will be produced for those tissues that do not respond. Failure of the drug to generate a change in motility over time with a characteristic spectrogram will likely predict resistance of that patient's tumor to that drug.

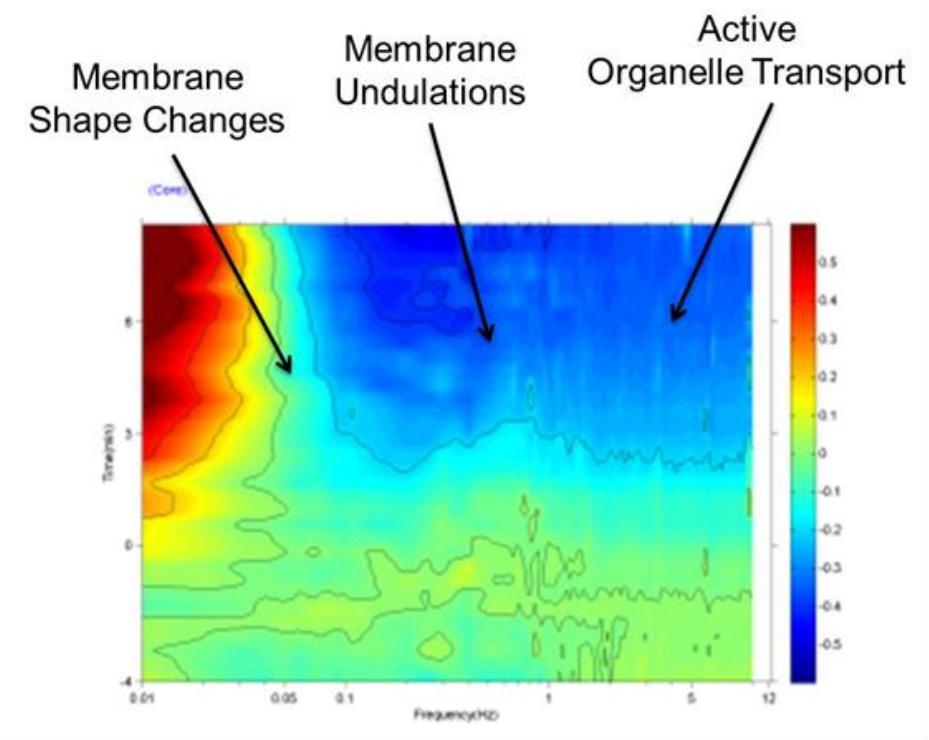

Figure 3 Sample drug-response spectrogram describing changes in various types of intracellular motion within a tumor over time following application of a drug at time = 0. Time is on the y-axis and the frequency of motion recorded is on the x-axis. Low-frequency motion, (such as membrane blebbing or rupture, associated with apoptosis or necrosis, respectively) is measured on the left side of the x-axis, medium-frequency motion (such as small cell membrane undulations) is measured in the middle of the x-axis, and high-frequency motion (such as that associated with internal organelle movements) is measured on the right side of the x-axis. The false color scale to the right describes increased motion as red and decreased motion as blue. This spectrogram shows a drug response in which low-frequency motility increases over time, while mid- and high-frequency motility decrease over time following drug exposure – this is consistent with an apoptotic response by the tumor cells. (Image courtesy of Dr. David Nolte)

To date, BDI has been applied only to multicellular tumor spheroids grown in vitro and to tumor xenografts harvested from rodents and exposed to chemotherapy drugs ex vivo. There are no published data describing the use of BDI to predict responsiveness of a naturally-occurring small animal tumor to chemotherapy. However, in preparation for the work described later in this thesis, we acquired preliminary BDI data from tumor biopsies from dogs with multicentric lymphoma.

2.3 Preliminary BDI Data

Preliminary work using ex vivo canine lymphoma samples suggests that BDI can be successfully applied to drug sensitivity screening, and personalized medicine in this cancer. Figure 4 shows motility contrast images generated from BDI applied to canine lymphoma biopsy samples, specifically comparing unique images generated for two dogs, one whose cancer progressed despite being treated with chemotherapy compared to a dog whose cancer responded. The top two images in panel A were produced from a tumor biopsy from a dog with high-grade peripheral T-cell lymphoma. This dog's lymphoma progressed in the face of doxorubicin in vivo. In contrast, the images on the bottom of panel A were made from a tumor biopsy from a dog with diffuse large B-cell lymphoma; this dog's lymphoma went into complete remission following doxorubicin chemotherapy in vivo. All biopsy samples were imaged pre- and post-treatment with doxorubicin (10 μM) ex vivo. As can be seen in Figure 4, the effects of ex vivo doxorubicin treatment were dramatically different between the doxorubicin-resistant T-cell lymphoma and the doxorubicin-sensitive B-cell lymphoma. There was a dramatic reduction in intracellular motility observed in the biopsy sample from the dog with the B-cell lymphoma, whereas there was no appreciable reduction in intracellular motion observed in the biopsy sample from the dog with the T-cell lymphoma. This same phenomenon is depicted in graph form in panel B of Figure 4.

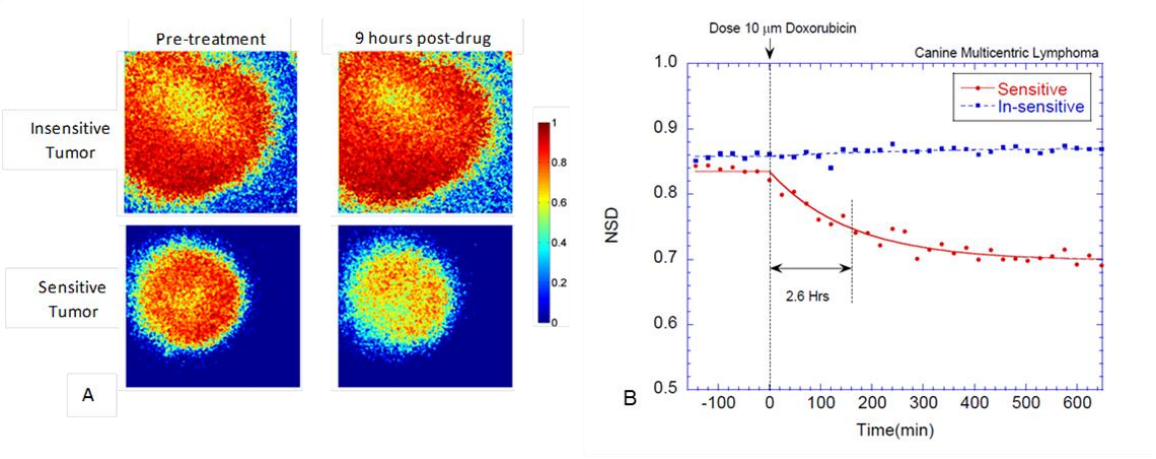

Figure 4 Panel A shows motility contrast images of tumor biopsy samples from two dogs with multicentric lymphoma. Biopsy samples were exposed to doxorubicin (10 μM) ex vivo, and images were taken both pre- and post-treatment. A false color scale to the right describes a motility metric (NSD) for each pixel in the images, with red areas corresponding to areas of greater cellular motility, and blue areas corresponding to areas of lesser cellular motility. The images at the top of the figure depict a tumor in which motility was not appreciably altered by ex vivo doxorubicin treatment. This dog's lymphoma progressed in the face of doxorubicin chemotherapy in vivo. The images at the bottom of the figure depict a tumor in which intracellular motility was significantly decreased following ex vivo doxorubicin treatment. This dog's lymphoma went into complete remission when treated with doxorubicin chemotherapy in vivo. Panel B depicts change in NSD values for the sensitive (red line) and insensitive (blue line) tumors graphically, with NSD plotted on the y-axis and time plotted on the x-axis. This figure demonstrates the significant reduction in intracellular motion in the sensitive tumor relative to the insensitive tumor following ex vivo application of doxorubicin.

BDI was also used to create drug response spectrograms describing the more detailed aspects of the change in intracellular motility in lymphoma biopsy samples exposed to doxorubicin ex vivo. Figure 5 depicts drug response spectrograms specific to the previously described doxorubicin-resistant T-cell lymphoma and doxorubicin-sensitive B-cell lymphoma. As can be seen from these images, ex vivo treatment with doxorubicin produces markedly different drug response spectrograms in the two samples. In the dog with B-cell lymphoma which clinically responded to doxorubicin, exposure of the biopsy samples to doxorubicin enhanced low frequency motion and suppressed high frequency

motion, similar to what is depicted in Figure 3. This spectrogram is associated with an apoptotic response to chemotherapy. In the biopsy sample from the dog with T-cell lymphoma which did not clinically respond to doxorubicin, doxorubicin exposure elicited comparatively little change in intracellular motion, potentially predicting the insensitivity of this tumor to chemotherapy.

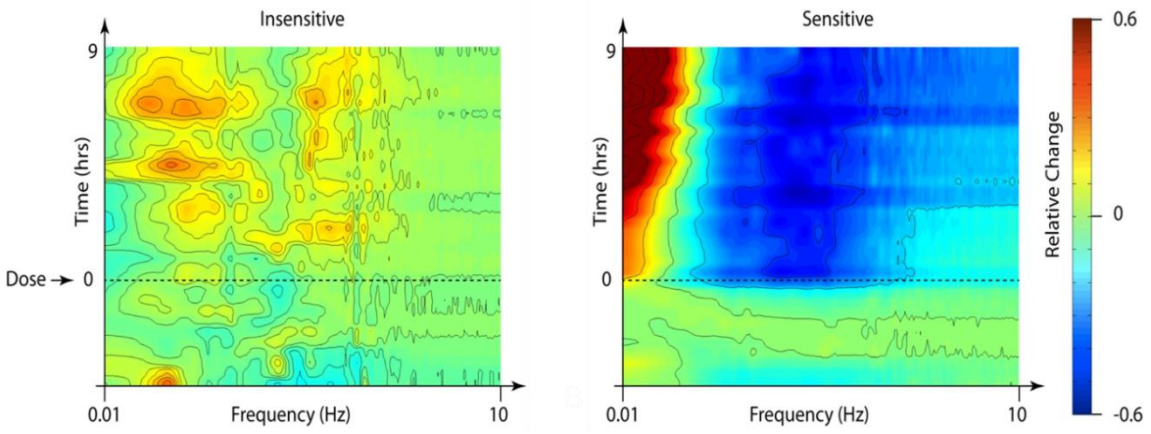

Figure 5 Drug response spectrograms generated using BDI on lymphoma biopsy samples from two different dogs. Time is plotted on the y-axis and frequency of motion detected is plotted on the x-axis. False color scales to the right of each image describe a motility metric (NSD) for each pixel in the images, with red areas corresponding to areas of greater cellular motility, and blue areas corresponding to areas of lesser cellular motility. Both biopsy samples were treated ex vivo with doxorubicin (10 μM) at time = 0. The spectrogram in panel A shows minimal increase in low- and mid-frequency motion and essentially unchanged high-frequency motion over time, indicating that doxorubicin has minimal effect on intracellular motion in this tumor. This spectrogram corresponds to a dog whose lymphoma progressed in the face of doxorubicin chemotherapy in vivo. The spectrogram in panel B shows marked increase in low-frequency motion with marked suppression of mid- and high-frequency motion over time. This is consistent with apoptosis or necrosis in the cells within this tumor. This spectrogram corresponds to a dog whose tumor went into complete remission following doxorubicin chemotherapy in vivo.

2.4 Use of Dogs as a Model for Human Non-Hodgkin's Lymphoma

While BDI has been successfully used to characterize drug responses in tumor spheroids in vitro and biopsies from tumor xenografts ex vivo, it has not previously been applied for predicting treatment outcome in a spontaneous animal tumor model. Naturally-occurring non-Hodgkin's lymphomas (NHL) in dogs represent a highly suitable preclinical animal tumor model in which to evaluate the predictive power of BDI. NHL in dogs are common tumors with histopathologic, molecular, and clinical features strikingly similar to NHL in humans[7]. In both people and dogs, these cancers typically present with generalized peripheral lymphadenomegaly, with liver, spleen, and bone marrow also commonly affected. In addition, doxorubicin-based combination chemotherapy is the standard of care for dogs and people with NHL. As previously mentioned, rather than to cure cancer, as is the common practice in human oncology, the treatment goal is to induce durable cancer remission and afford long-term disease palliation in dogs. Important clinical endpoints can be more rapidly assessed in dogs than people with NHL – objective response (OR) to chemotherapy typically is evident within days of treatment, and progression-free survival time (PFST) following chemotherapy is approximately 4-9 months[21]. Moreover, as is the case with human cancers, spontaneous NHL in dogs are both biologically and clinically diverse, and both OR and PFST following chemotherapy vary dramatically between individual patients. Due to the similarities between human and canine NHL and the shorter time needed to assess

clinical endpoints of disease in dogs with NHL, dogs are an excellent model in which to investigate BDI as a predictive assay for personalized cancer therapy

CHAPTER 3. APPLICATION OF BIODYNAMIC IMAGING FOR PERSONALIZED CHEMOTHERAPY IN CANINE LYMPHOMA

3.1 Statement of Purpose

The purpose of this pilot study was to determine the extent to which BDI data, obtained by imaging tumor biopsies taken from dogs with NHL and treated with doxorubicin ex vivo, would predict OR and PFST following doxorubicin chemotherapy in vivo.

3.2 Materials and Methods

3.2.1 Study Animals

Ten dogs with untreated, naturally-occurring NHL were prospectively enrolled into this study. All animals were privately-owned pet dogs seen at the Purdue University Veterinary Teaching Hospital (PUVTH), and enrolled between August 2013 and March 2014. The study protocol was approved by the Purdue Animal Care and Use Committee, and written informed consent was obtained from the owners of all dogs prior to enrollment. Study eligibility was based upon a clinical presentation consistent with primary nodal NHL and fine needle aspirate cytologic evaluation of an affected lymph node consistent with intermediate-to-high grade lymphoma. Additional inclusion criteria included body weight >15 kg, presence of at least one peripheral lymph node with longest diameter ≥ 2.5 cm, and expected survival of ≥4 weeks with treatment. Exclusion criteria included primary extranodal NHL, neutrophils <2,500 µl, platelets <100,000 µl, clinically significant cardiac dysfunction (defined as any ventricular arrhythmia, atrioventricular block, cardiomyopathy, congestive heart failure, or other cardiac conditions which would reasonably preclude doxorubicin treatment), clinically significant hepatic dysfunction (defined as serum alanine aminotransferase activity ≥4X upper limit of normal, hyperbilirubinemia, or serum biochemical evidence of hepatic synthetic failure), and prior treatment of any kind for the lymphoma.

3.2.2 Clinical Staging and Treatment of Study Animals

At the time of study enrollment, all dogs underwent surgical biopsy of an affected peripheral lymph node to provide material for histopathologic confirmation of NHL and for BDI. Nine dogs underwent incisional wedge biopsy of an affected lymph node, while one dog underwent multiple core biopsies using a 12 gauge biopsy needle (Magnum® disposable needle (12 G x 10 cm), Bard Medical). A portion of each dog's biopsy tissue (approximately 125 mm^3) was transferred to RPMI 1640 (Mediatech, Inc.) and submitted for BDI, while the remainder was fixed in 10% neutral buffered formalin and submitted for histopathologic evaluation. All lymphomas were histopathologically subtyped according to World Health Organization (WHO) criteria[22], based upon histomorphology in hematoxylin and eosin-stained tissue sections as well as immunohistochemical detection of CD3 or CD79a, as previously described[23]. All dogs underwent standardized cancer staging tests, including complete blood count, serum biochemistry profile, thoracic radiography, abdominal ultrasonography, bone marrow aspirate cytology, and electrocardiogram. All dogs were assigned a tumor stage based upon WHO criteria[24]. Following completion of staging tests, all dogs were scheduled to receive single-agent doxorubicin chemotherapy at a dose of 30 mg/m^2 administered intravenously once every 3 weeks for a maximum of 5 doses. While doxorubicin-based combination chemotherapy is considered standard for dogs with nodal NHL, single-agent doxorubicin treatment is a well-accepted and efficacious alternative to combination drug therapy[25,26]

3.2.3 Assessment of Clinical Endpoints

Caliper-based measurement of peripheral lymph nodes was used to assess objective response (OR) to chemotherapy, in accordance with criteria established by Vail, et al[27]. Briefly, complete remission (CR) was defined as the absence of measurable tumor burden; partial remission (PR) was defined as ≥30% reduction in the size of measurable tumor lesions; progressive disease (PD) was defined as ≥20% increase in the size of measurable tumor lesions, or the appearance of new lesions; and stable disease (SD) was defined as measurable tumor burden which was neither PR nor PD. OR was assessed once every three weeks during the course of treatment, and then once monthly following completion of treatment. Exceptions to this protocol were allowed if rapid disease progression necessitated prompt medical attention during the interval between scheduled rechecks. Progression-free survival time (PFST) was defined as the time elapsed between administration of the first doxorubicin treatment and the first detection of PD, or death due to any cause, whichever came first. All dogs were considered off study at the time that PD was first detected. Given that treatment outcome of canine NHL is strongly dependent upon the ability of chemotherapy to induce PR or CR early in the course of therapy, owners of dogs experiencing SD following the first dose of doxorubicin were given the option to withdraw their dogs from the study in order to pursue alternative treatment options.

3.2.4 Biodynamic Imaging

At the time of study enrollment, a portion of each dog's biopsy was placed in RPMI 1640 and transported immediately to a nearby laboratory for BDI. Each dog's biopsy was processed into approximately 16 (range 8-32) individual tissue samples of approximately 1 mm^3 size. These samples were mounted in in 8-well biomicroscopy slides (Lab-Tek), with each well containing several tumor samples. A thin layer of low-gel temperature porous agarose (Sigma-Aldrich) immobilized the tumor samples within the wells, and all samples were then overlaid with RPMI 1640. BDI was subsequently performed on all tissue samples, using previously described methods[15-17,19,20]. A schematic diagram of the BDI instrument is provided in Figure 6. The BDI system is a short-coherence Mach Zender interferometer with digital holographic acquisition and reconstruction. The three-dimensional capabilities are provided by coherence-gated detection that is equivalent to laser ranging using time-of-flight detection of backscattered light

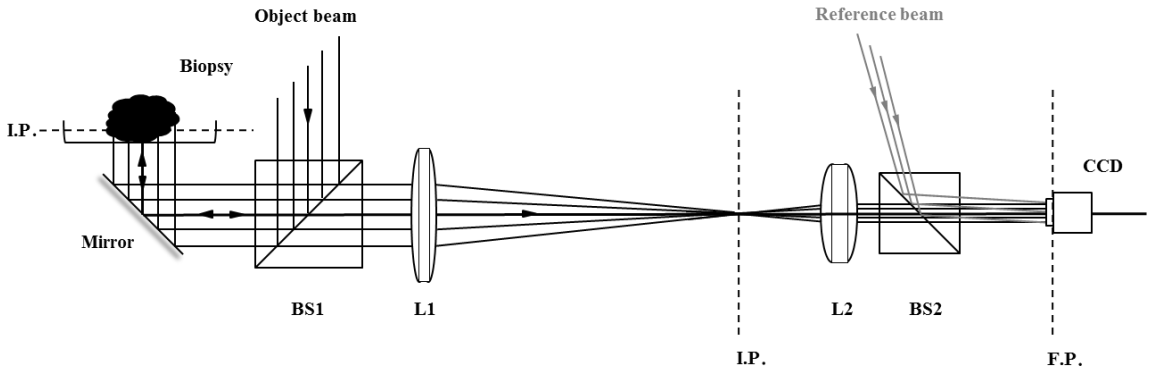

Figure 6 Schematic diagram of the BDI instrument. Low-coherence light is provided by a super luminescent diode (SLD, not depicted in the figure). A polarizing beam splitter separates light from the SLD into an object beam and a reference beam. The object beam is projected onto the tumor sample, and back scattered light from the tumor sample is Fourier transformed by the lenses (L1 and L2) before interfering with the reference beam at the Fourier plane (FP) of the object beam. Interference of the object beam with reference beam produces a speckle pattern which changes over time as a function of dynamic cellular motion within the tumor sample. The speckle pattern is captured by a charge-coupled device (CCD) camera as a reconstructed digital hologram for subsequent image analysis. BS = Beam splitter, IP = Image plane.

Baseline BDI data were recorded from all samples in each dog for approximately 4 hours, and then doxorubicin (10 μM) was applied to all samples. The concentration of doxorubicin applied is comparable to that which is achievable in plasma following intravenous administration of clinically-relevant doses of doxorubicin to dogs[28,29]. Following ex vivo doxorubicin treatment, BDI was performed continuously on all samples for approximately 9 hours. Motility contrast images[15-17] and drug response spectrograms [16-19] were acquired from all tissue samples using BDI. Motility contrast images are spatial maps of temporal fluctuations at a fixed depth inside the tissue set by the coherence gate (typically 400 microns inside the sample). Drug response spectrograms are time-frequency representations of the change in fluctuation of spectral

content in response to an applied drug. The frequency range spans from 0.01 Hz to 12.5 Hz.

Dynamic motility biomarkers measured by BDI included: 1.) *Baseline normalized standard deviation (NSD),* which describes baseline aggregate pixel intensity in motility contrast images, averaged over time; 2.) *Change in NSD from baseline (ΔNSD),* which describes the change in aggregate pixel intensity in motility contrast images, averaged over time, following ex vivo doxorubicin application; 3.) *Blue tail (BLUTAIL),* which describes the extent to which marked reduction in cellular motion was apparent in any of the samples at any frequency on drug response spectrograms; 4.) *Mid-frequency assessment (MEM),* which describes changes in motion apparent within the middle frequency range (0.1 Hz to 1 Hz) on drug response spectrograms; 5.) *Non-linear frequency assessment (APOP),* which describes changes in motion occurring at both high (> 1 Hz) and low (< 0.1 Hz) frequencies in drug response spectrograms, and for which specific spectral patterns have previously been correlated with an apoptotic response[17,18] and 6.) *All frequencies (ALLF),* in which data from the full frequency range (0.01 Hz to 12.5 Hz) are considered collectively. To account for heterogeneity in cellular and subcellular motility within the biopsy samples, data from each dog's biopsy samples were averaged to generate mean biomarker values for each dog. Mean biomarker values were used for all subsequent statistical analyses.

3.2.5 Statistical Analysis

Descriptive statistics, including best OR to chemotherapy and PFST, were recorded for each dog. The Kaplan-Meier method was used to generate survival curves and estimate median PFST for responders and non-responders. For the purposes of analysis, OR was dichotomously classified as either response (CR) or non-response (PR, SD, PD) to doxorubicin. A multivariate logistic model describing the correlation of averaged BDI data from each dog with OR and PFST was constructed. To allow PFST, a continuous variable, to be treated as a binary variable in the logistic model, the PFST values for all ten dogs were analyzed using k-means clustering, and the values were segregated into two groups based upon clustering results. Five of the six BDI-measured biomarkers (ΔNSD, BLUTAIL, MEM, APOP, and ALLF) were entered into the model and then the model was adjusted using backwards elimination. The values of all 5 biomarkers are given in Table 1. Each biomarker has been adjusted to zero mean and unity standard deviation across all 10 dogs.

Table 1 Five dynamic motility biomarkers for responsive (6) and non-responsive (4) dogs. Each biomarker has zero mean and unity standard deviation across all 10 dogs. The standard deviations of the biomarkers among the non-responsive dogs are smaller than for the responsive dogs. The biomarkers used in Fig. 12 are APOP, MEM, and BLUTAIL. The mean values and standard deviations from these three biomarkers are used to construct the input argument to the logistic function.

Responsive

Dog	**APOP**	**ALLF**	**MEM**	**BLUTAIL**	**ΔNSD**
1	-2.50	-2.20	-2.30	-1.70	-0.76
3	-0.24	-0.62	-0.17	-1.60	-1.58
5	0.00	0.88	0.16	0.52	0.79
6	-0.72	-1.10	-0.88	-0.98	-0.91
7	0.39	-0.05	0.32	0.86	0.87
9	0.40	0.13	-0.57	-0.29	-1.00
Avg	-0.44	-0.49	-0.57	-0.53	-0.43
Std	1.09	1.07	0.96	1.08	1.02

Non-Responsive

Dog	**APOP**	**ALLF**	**MEM**	**BLUTAIL**	**ΔNSD**
2	0.07	1.30	1.40	0.72	1.28
4	1.00	0.70	0.56	0.83	-0.06
8	0.46	0.20	0.47	0.78	0.12
10	1.20	0.77	1.00	0.84	1.12
Avg	0.68	0.74	0.86	0.79	0.62
Std	0.52	0.45	0.43	0.06	0.68

The argument to the logistic function is constructed from the mean values and standard deviations of these biomarkers to construct a multivariable logistic predictor of drug response as:

$$L_n = \text{logistic}\left[\sum_{m=1}^{M} \frac{(b_{nm} - B_m)}{\sigma_m}\right]$$

Where L_n is the logistic drug response predictor for the n^{th} dog, m varies over the selected biomarkers, M is the number of biomarkers, b_{nm} is the value of the m^{th} biomarker for the

n^{th} dog, σ_m is the standard deviation of the m^{th} biomarker, and B_m is the binary threshold between the two populations (responsive and non-responsive) for the m^{th} biomarker. To account for possible over-fitting of clinical data to the model, cross-validation using one-left-out analysis was also performed. The logistic values for the responder and non-responder populations were fitted with a continuous-valued Gaussian distribution to generate a receiver operating characteristic curve in order to calculate sensitivity, specificity, and accuracy of BDI for predicting treatment outcome.

3.3 Results

Eight dogs with B-cell NHL and two dogs with T-cell NHL were enrolled. Seven of the eight dogs with B-cell NHL had DLBCL, while in the eighth dog, WHO subtyping was not performed because the biopsy method (needle core) provided inadequate tissue for this purpose. Both dogs with T-cell NHL had PTCL-NOS. Doxorubicin chemotherapy was tolerated well by all dogs, and treatment-related adverse events were mild, in keeping with previous reports[37, 38]. Demographic and treatment response data are summarized in Table 2. Objective response to chemotherapy was classified as response in 6 dogs experiencing CR of their NHL, and non-response in 4 dogs experiencing PR (1), SD (2) or PD (1). Two responder dogs were still alive with their NHL in CR at the time of data analysis. A Kaplan-Meier plot describing cumulative PFST over the study period in responder vs. non-responder dogs is presented in Figure 7.

Table 2 Demographic and treatment response variables for 10 dogs with naturally occurring non-Hodgkin's lymphomas treated with single-agent doxorubicin chemotherapy. WHO – World Health Organization; DLBCL – Diffuse large B-cell lymphoma; PTCL-NOS – Peripheral T- cell lymphoma, not otherwise specified; OR – best objective response to chemotherapy; CR – complete remission; PR – partial remission; SD – stable disease; PD – progressive disease; PFST – progression-free survival time; N/A – Not evaluable due to biopsy method (needle core).

Dog	**Breed**	**Tumor Immunophenotype**	**WHO subtype**	**WHO Stage**	**OR**	**PFST (days)**
1	Golden retriever	B-cell	N/A	5	CR	154
2	Boxer	B-cell	DLBCL	4	PR	37
3	Mixed	B-cell	DLBCL	4	CR	301
4	Mixed	B-cell	DLBCL	4	SD	21
5	Mixed	B-cell	DLBCL	4	CR	174
6	Labrador retriever	B-cell	DLBCL	4	CR	180
7	Golden retriever	B-cell	DLBCL	4	CR	>196
8	Mixed	T-cell	PTCL-NOS	5	PD	21
9	Mixed	B-cell	DLBCL	4	CR	>176
10	Rhodesian ridgeback	T-cell	PTCL-NOS	5	SD	22

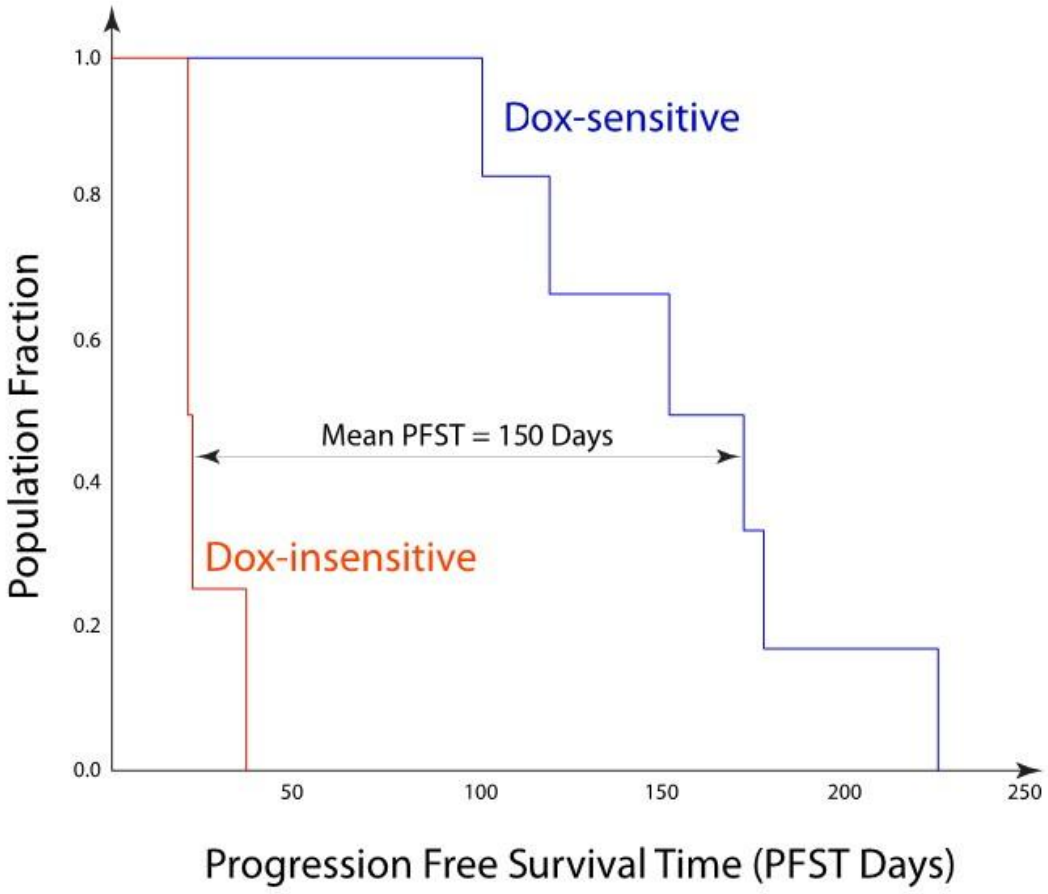

Figure 7 Kaplan-Meier plot describing progression-free survival time (PFST) in 10 dogs with NHL treated with single-agent doxorubicin chemotherapy. Cumulative PFST for responder dogs (Dox-sensitive) is plotted in blue, and that for non-responder dogs (Dox-insensitive) is plotted in red.

Representative averaged motility contrast images generated by BDI on biopsy samples obtained from two study dogs are depicted in Figure 8. Many of the tumor biopsy samples from the dogs which were responsive to doxorubicin in vivo showed a dramatic reduction in aggregate intracellular motility following ex vivo application of doxorubicin. In contrast, in tumors from dogs which were non-responsive to doxorubicin

in vivo, nearly all biopsy samples demonstrated minimal change in aggregate intracellular motility following ex vivo doxorubicin treatment. Figure 9 shows the averaged NSD values of tumor biopsies for the responsive and non-responsive populations plotted as a function of time. The mean decrease in NSD for tumors from responsive dogs was $\Delta NSD = -0.55$, and that for tumors from non-responsive dogs was $\Delta NSD = -0.13$. Therefore, following ex vivo application of doxorubicin, a drop in NSD from baseline was apparent in tumors from the dogs experiencing CR of their NHL to doxorubicin in vivo. In contrast, NSD did not deviate substantially from baseline in tumors from the dogs experiencing PR, SD, or PD of their NHL following doxorubicin chemotherapy.

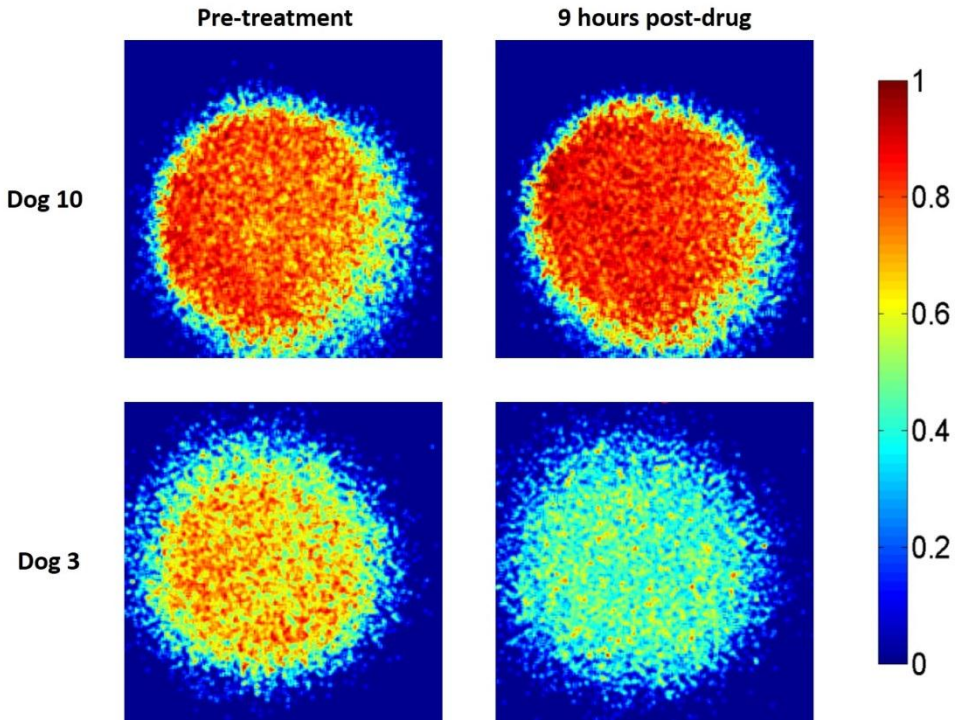

Figure 8 Characteristic motility contrast images, which depict aggregate cellular motion averaged over time, of tumor biopsy samples obtained from two dogs with NHL. The two images in the top row depict a tumor from a non-responder dog (Dog 10) in which aggregate cellular motion was unaltered to slightly increased following ex vivo doxorubicin treatment. The two images in the bottom row depict a tumor from a responder dog (Dog 3) in which aggregate cellular motion was markedly decreased following ex vivo doxorubicin treatment.

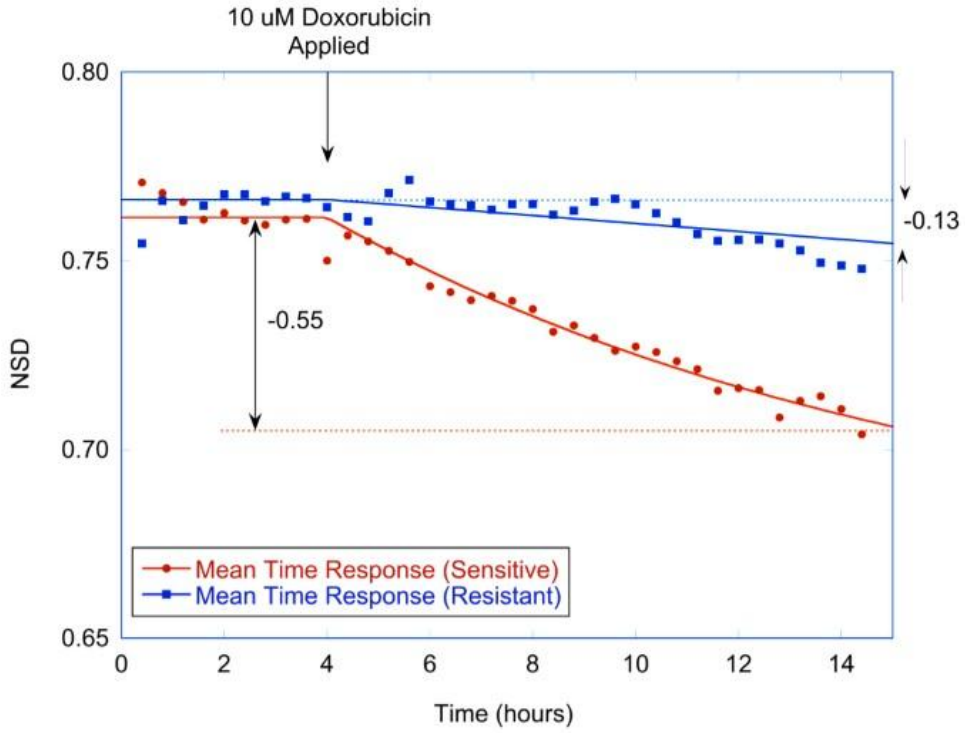

Figure 9 Graphical representation of change in aggregate cellular motion (ΔNSD) following ex vivo application of doxorubicin to tumor biopsies taken from all 10 study dogs. Mean NSD (y-axis) for the 6 responder dogs (red line) and 4 non-responder dogs (blue line) is plotted as a function of time (x-axis). The mean ΔNSD for the 6 responder dogs (-0.55) was greater than that for the 4 non-responder dogs (-0.13).

Representative drug response spectrograms generated by BDI on tumor biopsy samples obtained from study dogs are depicted in Figures 10 and 11. Figure 10 shows a schematic representation of how spectral signatures generated by imaging all twelve of the 1 mm^3 biopsy samples obtained from an individual dog's (Dog 9) tumor were merged to create an averaged spectrogram. Figure 11 shows averaged drug response spectrograms from two different dogs with NHL. Panel A of the figure depicts an averaged drug response spectrogram for a non-responsive dog (Dog 10), in which motions at all frequencies are essentially unchanged or slightly enhanced following ex

vivo application of doxorubicin; this spectrogram corresponds to a dog that experienced PD of its NHL following doxorubicin treatment in vivo. Panel B depicts an averaged drug response spectrogram from a responsive dog (Dog 9), in which motions at all recorded frequencies are significantly suppressed following ex vivo application of doxorubicin; this spectrogram corresponds to a dog that experienced CR of its NHL following doxorubicin treatment in vivo.

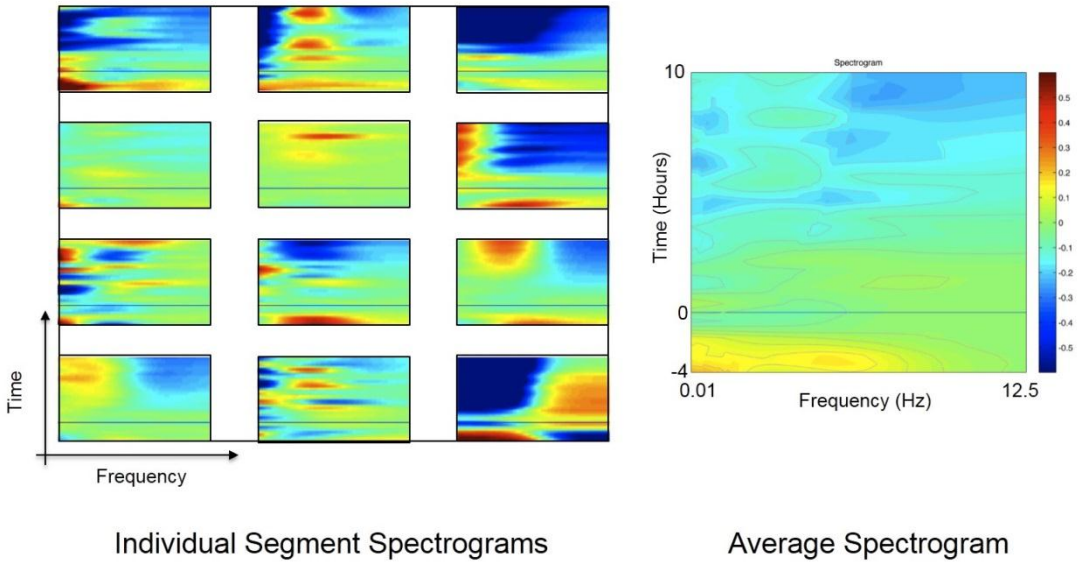

Figure 10 Drug response spectrograms depicting alterations in various aspects of cellular and intracellular motion occurring across a range of frequencies over time in ex vivo tumor biopsies from a dog (Dog 9) with NHL. Frequency of motion detected is plotted on the x-axis of each panel and time is plotted on the y-axis. BDI generated a unique drug response spectrogram from each of the 12 tumor biopsy samples from this dog. There is marked variability in spectral data obtained by imaging each biopsy sample, and thus data from all 12 spectrograms were averaged (larger panel on the right side of the figure) for the purposes of statistical analysis.

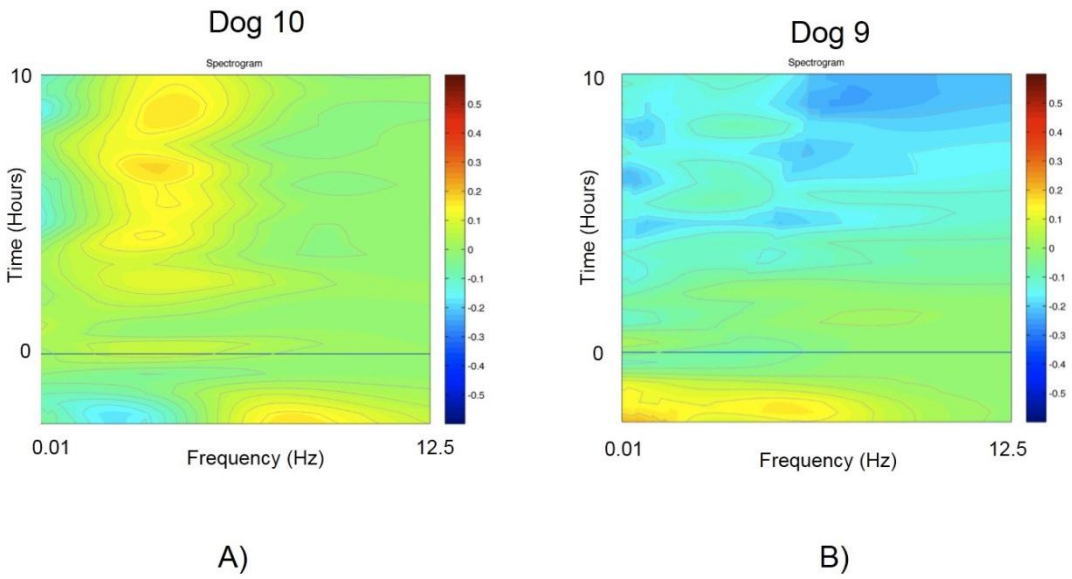

Figure 11 Characteristic averaged drug response spectrograms from a non-responder dog (Dog 10; Panel A) and a responder dog (Dog 9; Panel B). Frequency of motion detected is plotted on the x-axis, and time is plotted on the y-axis in each panel. Doxorubicin (10 μM) was applied at time = 0.

K-means clustering of the 10 dogs according to PFST showed the 4 non-responder dogs to cluster around a PFST of approximately 20-30 days, while the 6 responder dogs clustered around a PFST of >100 days; therefore, in this population of dogs, the binary classification of response vs. non-response was the same regardless of whether OR or PFST was the basis for classification. Results of the multivariate logistic analysis are depicted graphically in Figure 12 (solid color bars). The average logistic values for each population (responsive and non-responsive are shown as dashed lines on the graph. Using backwards elimination, a logistic model was constructed which incorporated three biomarkers (M=3): nonlinear (APOP), mid-frequency (MEM), and blue tail (BLUTAIL). These three metrics correlated most strongly with PFST and OR. By combining the three biomarkers in a multivariate logistic function, the combined

group predicted OR to doxorubicin chemotherapy in 100% of cases using a binary classifier (response vs. non-response) that fully separates the two groups. The separation (±SD) between the mean values of the two groups is 0.73 (±0.39). The sensitivity, specificity, and accuracy for the complete data set in Figure 6 are 95%, 91%, and 93%, respectively. To test against over-fitting, cross-validation with a one-left out analysis was performed. Thresholds for the binary classifier were set using nine of the ten dogs, and then the tenth dog was tested against the classifier. This procedure was repeated for each dog. The response of each left-out dog is plotted in Figure 12 as the half-tone bars. Dog 7 had a weak sensitive signature in the full set, but was classified as resistant in the one-left-out analysis. The sensitivity, specificity, and accuracy for this combination of three dynamic motility metrics were 93%, 87%, and 91%, respectively. Increasing the number of biomarkers in the logistic model improved the accuracy for the full set, but beyond the optimum combination, the one-left-out analysis became less accurate. Therefore, in this study, the optimum combination was provided by the three biomarkers most representative of overall response.

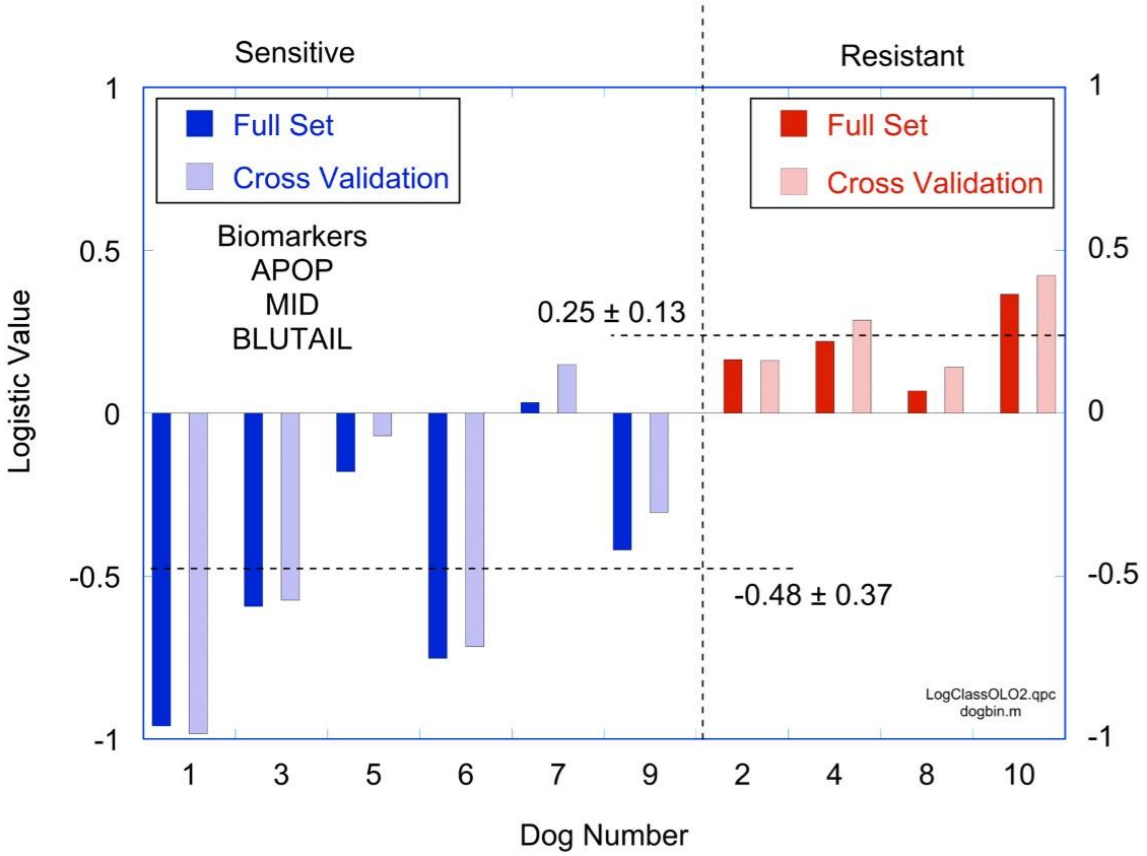

Figure 12 Graphical representation of the relationship between BDI data and treatment outcome in 10 dogs with NHL. Individual dogs are plotted on the x-axis and the value of the logistic drug response predictor is plotted on the y-axis. Blue bars denote responder dogs (sensitive) and red bars denote non-responders (resistant). Solid color bars denote the results of initial multivariate logistic modeling and the half-tone bars denote the results of cross-validation with one-left-out analysis.

CHAPTER 4. CONCLUSION

In this report, we show for the first time that a novel live-tissue imaging technology, BDI, can be effectively use to predict treatment outcome with high accuracy following doxorubicin chemotherapy in a relevant, naturally-occurring animal model of non-Hodgkin's lymphoma. Although the sample size of 10 dogs in this study was small, the lymphoma in the 10 dogs was fairly representative for NHL in dogs as a whole. Approximately 75-80% of NHL in dogs are B-cell tumors, and the remaining 20-25% are T-cell tumors. Tumor immunophenotype is among the most powerful predictors of therapeutic response in dogs with NHL, in that dogs with T-cell NHL typically experience less robust and less durable responses to doxorubicin-based chemotherapy than dogs with B-cell NHL[32-34]. When treated with single-agent doxorubicin, fewer than 20% of dogs with T-cell NHL will experience CR of their lymphoma; in contrast, over 80% of dogs with B-cell NHL experience CR following doxorubicin treatment[32]. Thus, the poor response to doxorubicin chemotherapy in the two dogs with T-cell NHL in this study could have been predicted to some degree based upon immunophenotype alone. Nevertheless, BDI accurately predicted response to doxorubicin in these two dogs. Perhaps more significantly, BDI accurately identified the 2/8 dogs with B-cell NHL which would fail to exhibit CR to doxorubicin chemotherapy despite belonging to a

prognostically favorable subgroup. Although these data require confirmation in a larger sample set, they suggest that BDI may more accurately predict response to therapy in this dog model of NHL than is possible using traditional clinical or pathological indices.

This predictive capability of BDI sets it apart from other real-time living tissue imaging modalities which have recently emerged as tools for the clinical evaluation of cancer. Among these are confocal laser endomicroscopy, narrow band imaging, Raman laser spectroscopy, and optical coherence tomography (OCT) [35-39]. By evaluating alterations in tissue structure and chemical composition, these techniques can distinguish cancerous tissues from normal ones at the histologic level with excellent accuracy. To date, these techniques have been applied most commonly to cancer detection, and can be used to reveal occult premalignant lesions, to discern cancerous from precancerous lesions, or to measure minute tumor volumes. OCT has also been used to characterize tumor response to therapy in preclinical models by measuring changes in tumor volume or vascularity following anti-angiogenic drug treatment[39]. BDI shares many features with OCT – for example, both rely upon collection of back-scattered short-coherence light to define depth and spatial resolution within tissues. However, the reconstructed images produced by BDI are a product of dynamic coherent speckle of the back-scattered light. Coherent speckle results from interference of many light waves with similar frequency, but with different phases and amplitudes, which superpose to produce a complex wavefront of randomly varying amplitude and intensity. This speckle effect is detrimental to OCT because it limits optical resolution and blurs the boundaries between microanatomical planes[40], but it is essential to BDI because it provides contrast by which to discern dynamic changes in cellular and subcellular motion within 3-dimensional

tissues in response to drugs. By analyzing temporal fluctuations in dynamic cellular motion within drug-treated tumor tissue samples, BDI defines physiologic rather than anatomic properties of tumors. Therefore, whereas other real-time tumor imaging technologies have been largely applied as diagnostic tools, BDI can function as a predictive tool in cancer medicine.

This predictive ability of BDI suggests its possible application to PCM. BDI may have some advantages over previously described PCM assays, which generally attempt to predict response to therapy by characterizing genotypic derangements within individual patients' tumors. As such, existing PCM assays attempt to correlate genotypic data, such as patterns of gene expression or presence of well-characterized gene mutations, with a phenotypic response, i.e. tumor remission. But while it is genes and proteins which provide the blueprints and structural framework for living cells, the ultimate phenotypic expression of all cellular activity is motion. By phenotypically profiling tumors using detailed probing of cellular and subcellular motion, BDI may have significant potential to enhance the prediction of tumor response to drug therapy and inform the selection of optimal treatments for individual patients relative to what is possible using genotypic PCM approaches. For example, while molecularly-targeted therapies, such as BRAF inhibitors in patients with melanoma bearing the V600E mutation[41] or ALK inhibitors in patients with non-small cell lung cancer bearing ALK/EML4 translocations[42], afford high initial response rates, cancer resistance to these therapies usually develops within several months. Moreover, druggable molecular targets are not identifiable using genotypic methods on tumors from many patients at the time of cancer diagnosis[43,44]. A phenotypic profiling method, such as BDI, may be useful for selecting drugs for patients in which

targeted therapy has failed or whose tumors do not express a known molecular target for drug therapy, in that BDI could predict phenotypic response in the absence of validated genotypic biomarkers. While the present study involved the treatment of a spontaneous animal tumor with doxorubicin, a non-targeted drug, BDI has been used to evaluate the effects of targeted drugs in in vitro models[19]. It is therefore plausible that BDI would be useful to predict phenotypic response to targeted and non-targeted therapies in human cancer patients by imaging tumor biopsy samples ex vivo, such as was described in the present study.

The three dynamic biomarkers most predictive of overall response in this study were APOP, MEM, and BLUTAIL. APOP is a signature correlated with apoptosis[17], which is a desired outcome of cancer therapy. MEM is related to membrane transport, which can exhibit activation upon exposure of neoplastic tissues to chemotherapy, and is possibly reflective of active drug transport by membrane-associated efflux proteins induced as a protective strategy for cancer cells. BLUTAIL specifically measures the presence of a subset of biopsy samples that show strong inhibition of motion in response to therapy, even if the response averaged over all the tumor samples is weak. These three dynamic biomarkers have specific connections with the physiological response of tissues to applied anti-proliferative or cytotoxic drugs.

While predicting clinical response to doxorubicin in the dogs in this study was possible using these three biomarkers, considerable heterogeneity in cellular motility was observed in processed biopsy samples from all dogs, both prior to and following ex vivo application of doxorubicin (Figure 10). This may be due to inherent biological heterogeneity of the neoplastic cell population comprising individual dogs' tumors. It is

well documented that tumors are composed of heterogeneous subpopulations of cells with distinct genomic identities and functional properties[45,46]. It is likely that these subpopulations exhibit variable motility profiles as well. However, another possible explanation for the heterogeneity in motility profiles within each tumor sample could be that motility varied based upon histologic composition of the tissue (i.e. tumor cells vs. stroma) or tissue viability (i.e. live tumor cells vs. apoptotic or necrotic cells). We attempted to account for heterogeneity in cellular motion by averaging motility metrics from all processed biopsy samples in each patient, and submitting the averaged data to statistical analysis. Future investigations are needed to determine the optimal number of samples to be analyzed in order to maximize the predictive power of BDI, and to better define the mechanisms underlying the heterogeneous motility profiles observed within processed biopsy samples from the same tumor. Because BDI is performed on minimally disrupted living tissue, it also could be easily paired with post-hoc assays to determine the extent to which motility differences (in untreated tissue samples) correlate with genomic and proteomic alterations within multiple, anatomically confined regions of a tumor. Furthermore, post-hoc histopathologic evaluation of tumor tissues, which was not part of the current study design, would be an invaluable component of future studies to evaluate whether tissue composition is a significant determinant of heterogeneous motility properties within ex vivo tumor biopsy samples.

The data presented here provide proof-of-concept to justify further investigation of BDI as a viable method for personalized cancer therapy. The most significant limitations of the present study include its small sample size and that only a single drug was investigated. These data require confirmation in a larger study population and in the

context of multiple or combination drug therapies. Nonetheless, these results suggest that BDI may have significant power to predict tumor response to chemotherapy a priori, and could therefore serve as an important tool for therapeutic drug selection in individual cancer patients.

WORKS CITED

WORKS CITED

1.) Dorn CR, Taylor DON, and Schneider R. The epidemiology of canine leukemia and lymphoma. Bibl Haematol 1970;36:403-415.

2.) Priester WA, McKay FW. The occurrence of tumors in domestic animals. Natl Cancer Inst Monogr 1980;54:1-210.

3.) Garrett LD, Thamm DH, Chun R, Dudley R, and Vail DM. Evaluation of a 6-month chemotherapy protocol with no maintenance for dogs with lymphoma. J Vet Intern Med 2002;16:704-709.

4.) Zemann BI, Moore AS, Rand WM, et al. A combination chemotherapy protocol (VELCAP-L) for dogs with lymphoma. J Vet Intern Med 1998;12:465-470.

5.) Keller ET, MacEwen EG, Rosenthal RC, et al. Evaluation of prognostic factors and sequential combination chemotherapy with doxorubicin for canine lymphoma. J Vet Intern Med 1993;7:289-295.

6.) Carter RF, Harris CK, Withrow SJ, et al. Chemotherapy of canine lymphoma with histopathological correlation: doxorubicin alone compared to COP as first treatment regimen. J Am Anim Hosp Assoc 1987;23:587-596.

7.) Ito D, Frantz AM, Modiano JF. Canine lymphoma as a comparative model for human non-Hodgkin lymphoma: recent progress and applications. Vet Immunol Immunopathol. 2014;159192-201.

8.) Gonzalez de Castro D, Clarke PA, Al-Lazikani B, et al. Personalized cancer medicine: molecular diagnostics, predictive biomarkers, and drug resistance. Clin Pharmacol Ther 2013;93:252-259.

9.) Walther Z, Sklar J. Molecular tumor profiling for prediction of response to anticancer therapies. Cancer J. 2011;17:71-9.

10.) Alizadeh AA, Eisen MB, Davis RE, et al. Distinct types of diffuse large B-cell lymphoma identified by gene expression profiling. Nature 2000;403:503-511.

11.) Rosenwald A, Wright G, Chan W, et al. The use of molecular profiling to predict survival after chemotherapy for diffuse large B-cell lymphoma. N Engl J Med 2002;346:1937-1947.

12.) Hans CP, Weisenburger DD, Greiner TC, et al. Confirmation of the molecular classification of diffuse large B-cell lymphoma by immunohistochemistry using a tissue microarray. Blood 2004;103:275-282

13.) Chin L, Anderson JN, Futreal PA. Cancer genomics: from discovery science to personalized medicine. Nat Med. 2011;17:297-303.
14.) Junttila MR, deSauvage FJ. Influence of tumour micro-environment heterogeneity on therapeutic response. Nature. 2013;501:346-54.
15.) Jeong K, Turek JJ, Nolte DD. Volumetric motility-contrast imaging of tissue response to cytoskeletal anti-cancer drugs. Opt Express 2007;15:14057-14064.
16.) Nolte DD, An R, Turek J, Jeong K. Holographic tissue dynamics spectroscopy. J Biomed Opt 2011;16:087004.
17.) Nolte DD, An R, Turek J, Jeong K. Tissue dynamics spectroscopy for phenotypic profiling of drug effects in three-dimensional culture. Biomed Opt Express. 2012;3:2825-41.
18.) An R, Merrill D, Avramova L, Sturgis J, Tsiper M, Robinson JP, et al. Phenotypic profiling of Raf inhibitors and mitochondrial toxicity in 3D tissue using biodynamic imaging. J Biomol Screen. 2014;19:526-37.
19.) An R, Turek J, Matei DE, et al. Live tissue viability and chemosensitivity assays using digital holographic motility contrast imaging. Appl Opt 2013;52:A300-A309.
20.) Yu P, Peng L, Mustata M, et al. Time-dependent speckle in optical coherence imaging and health of tumor tissue. Opt Lett 2004;29:68-70.
21.) Garrett LD, Thamm DH, Chun R, Dudley R, Vail DM. Evaluation of a 6-month chemotherapy protocol with no maintenance for dogs with lymphoma. J Vet Intern Med. 2002;16:704-709.
22.) Valli VE, San Myint M, Barthel A, et al. Classification of canine malignant lymphomas according to the World Health Organization Criteria. Vet Pathol 2011;48:198-211.
23.) Ramos-Vara JA, Miller MA, Valli VE. Immunohistochemical detection of multiple myeloma 1/interferon regulatory factor 4 (MUM1/IRF-4) in canine plasmacytoma: comparison with CD79a and CD20. Vet Pathol. 2007;44:875-884.
24.) Owen LN. TNM classification of tumors in domestic animals. Geneva: World Health Organization; 1980.
25.) Carter RF, Harris CK, Withrow SJ, Valli VE, Susaneck SJ. Chemotherapy of canine lymphoma with histopathological correlation: doxorubicin alone compared to COP as first treatment regimen. J Am Anim Hosp Assoc. 1987;23:587-596.
26.) Mutsaers AJ, Glickman NW, DeNicola DB, Widmer WR, Bonney PL, Hahn KA, et al. Evaluation of treatment with doxorubicin and piroxicam or doxorubicin alone for multicentric lymphoma in dogs. J Am Vet Med Assoc. 2002;220:1813-7.

27.) Vail DM, Michels GM, Khanna C, et al. Response evaluation criteria for peripheral nodal lymphomas in dogs (v1.0) – a veterinary cooperative oncology group (VCOG) consensus document. Vet Comp Oncol 2009;8:28-37.
28.) Baldwin JR, Phillips BA, Overmyer SK, et al. Influence of the cardioprotective agent dexrazoxane on doxorubicin pharmacokinetics in the dog. Cancer Chemother Pharmacol 1992;30:433-438.
29.) Wilke AV, Jenkins C, Milligan AJ, et al. Effect of hyperthermia on normal tissue toxicity and on adriamycin pharmacokinetics in dogs. Cancer Res 1991;51:1680-1683.
30.) Teske E. Canine malignant lymphoma: a review and comparison with human non-hodgkin's lymphoma. Veterinary Quarterly 1994;16(4): 209-19
31.) Younes A, Berry DA. From drug discovery to biomarker-driven clinical trials in lymphoma. Nat Rev Clin Oncol 2012;9:643-653.
32.) Beaver LM, Strottner G, Klein MK. Response rate after administration of a single dose of doxorubicin in dogs with B-cell or T-cell lymphoma: 41 cases (2006-2008). J Am Vet Med Assoc. 2010;237:1052-5.
33.) Wilkerson MJ, Dolce K, Koopman T, Shuman W, Chun R, Garrett L, et al. Lineage differentiation of canine lymphoma/leukemias and aberrant expression of CD molecules. Vet Immunol Immunopathol. 2005;106:179-96.
34.) Ruslander DA, Gebhard DH, Tompkins MB, Grindem CB, Page RL. Immunophenotypic characterization of canine lymphoproliferative disorders. In Vivo. 1997;11:169-72.
35.) Liu J, Droller MJ, Liao JC. New optical imaging technologies for bladder cancer: considerations and perspectives. J Urol. 2012;188:361-8.
36.) Green B, Cobb AR, Brennan PA, Hopper C. Optical diagnostic techniques for use in lesions of the head and neck: review of the latest developments. Br J Oral Maxillofac Surg. 2014;52:675-80.
37.) Wang W, Zhao J, Short M, Zeng H. Real-time in vivo cancer diagnosis using raman spectroscopy. J Biophotonics. Epub 2014 Sep 12. PMID 25220508.
38.) Vakoc BJ, Fukumura D, Jain RK, Bouma BE. Cancer imaging by optical coherence tomography: preclinical progress and clinical potential. Nat Rev Cancer. 2012;12:363-8.
39.) Vakoc BJ, Lanning RM, Tyrrell JA, Padera TP, Bartlett LA, Stylianopoulous T, et al. Three-dimensional microscopy of the tumor microenvironment in vivo using optical frequency domain imaging. Nat Med. 2009;15:1219-24.
40.) Karamata B, Hassler K, Laubscher M, Lasser T. Speckle statistics in optical coherence tomography. J Opt Soc Am A. 2005;22:593-6.

41.) Flaherty KT, Puzanov I, Kim KB, Ribas A, McArthur GA, Sosman JA, et al. Inhibition of mutated, activated BRAF in metastatic melanoma. N Engl J Med. 2010;363:800-19.

42.) Kwak EL, Bang YJ, Camidge DR, Shaw AT, Solomon B, Maki RG, et al. Anaplastic lymphoma kinase inhibition in non-small-cell lung cancer. N Engl J Med. 2010;363:1693-703

43.) Tsimberidou AM, Iskander NG, Hong DS, Wheler JJ, Falchook GS, Fu S, et al. Personalized medicine in a phase I clinical trials program: the MD Anderson Cancer Center initiative. Clin Cancer Res. 2012;18:6373-83.

44.) Tsimberidou AM, Wen S, Hong DS, Wheler JJ, Falchook GS, Fu S, et al. Personalized medicine for patients with advanced cancer in the phase I program at MD Anderson: validation and landmark analyses. Clin Cancer Res. 2014;20:4827-36.

45.) Snuderl M, Fazlollahi L, Le LP, Nitta M, Zhelyazkova BH, Davidson CJ, et al. Mosaic amplification of multiple receptor tyrosine kinase genes in glioblastoma. Cancer Cell. 2011;20:810-7.

46.) Gerlinger M, Rowan AJ, Horswell S, Larkin J, Endesfelder D, Gronroos E, et al. Intratumor heterogeneity and branched evolution revealed by multiregion sequencing. N Engl J Med. 2012;366:883-92.

VITA

VITA

Education

Diplomate Candidate (ACVIM, oncology), Purdue Veterinary Teaching Hospital, West Lafayette, IN (2012 –present)
Master of Science Candidate, Purdue Veterinary Teaching Hospital, West Lafayette, IN (2012 – present)
Thesis: *Application of Biodynamic Imaging for Personalized Chemotherapy in Canine Lymphoma: A Pilot Study*
Oncology Internship under Dr. Chand Khanna, The Oncology Service, Washington, DC (2011 – 2012)
Small Animal Rotating Internship, Garden State Veterinary Specialists, Tinton Falls, NJ (2010 – 2011)
Doctor of Veterinary Medicine, Virginia-Maryland Regional College of Veterinary Medicine, Blacksburg, VA (2006 – 2010)
Bachelor of Arts (biology), St. Mary's College of Maryland, St. Mary's City, MD (2002 – 2006)
Thesis: *Incidence and Prevalence of Hemoparasites in Wild-Caught Australian Turtles*

Veterinary-Related Experience

Clinical instructor: topics in medical oncology to 4th year veterinary students. Purdue University, West Lafayette IN (2012 – 2013)
Intern instructor: topics in medical oncology to veterinary interns. Purdue University, West Lafayette IN (2012 – 2014)
Research grant writer: collaborative, multi-disciplinary grants for personalized medicine assays. Purdue University, West Lafayette IN (2012 – 2013)
Clinical investigator: pharmaceutical/biotech veterinary oncology drug development projects. Animal Clinical Investigation, Washington DC (2011 – 2012)
Research proposal writer: dose escalation study of toremifene for the treatment of mammary gland adenocarcinoma in client-owned cats. Animal Clinical Investigation, Washington DC (2011)
Book chapter author: comparative biology of cancer metastasis (in preparation with Dr. Chand Khanna)

Professional Affiliations

American Association of Cancer Research, 2013 – 2014
American College of Veterinary Internal Medicine, 2012 – 2014
Veterinary Cancer Society, 2011, 2014
American Veterinary Medical Association: 2010, 2011
Student American Veterinary Medical Association: 2006 – 2011
Veterinary Business Management Association: 2007 – 2010

Academic Honors

Florence A. Nocka Endowed Award (2009)
Maryland Higher Education Commission Scholarship (2008)

Publications

Custead M et al. *Metronomic chlorambucil, a dose finding study in canine solid tumors.* JVIM, in preparation

Grants

Custead M and Childress M. *Application of Biodynamic Imaging for Personalized Chemotherapy in Canine Lymphoma: A Pilot Study*. Purdue Veterinary Clinical Science, Internal Resident Competitive Grant, 2014
Custead M and Childress M. *Application of Biodynamic Imaging for Personalized Chemotherapy in Canine Lymphoma: A Pilot Study*. ACORN Grant, AKC Canine Health Foundation, 2014

Free Communications

Custead M. 2013. *Personalized Medicine: Building Blocks in Veterinary Oncology.* Purdue Veterinary Seminar Series. West Lafayette, IN.
Custead M. 2013. *Metastasis Biology.* Purdue Veterinary Seminar Series. West Lafayette, IN.
Custead M. 2011. *Lyme disease, recent advances*. Northern New Jersey Continuing Education. Tinton Falls, NJ.
Custead M. 2008. *International student veterinary experience in the curriculum*. SCAVMA. Blacksburg VA.
Custead M. 2008. *Tackling the Everglades with Geographical Information Systems*. Envirovet Student Presentations. White Oak, FL.
Custead M. 2007. *Comparison of the prevalence of human clinical Chagas cases and confirmed triatominaes infected with trypanosomes using Geographical Information Systems in Itaberaba, Bahia***.** Universidade Federal da Bahia Escola de Medicina Veterinária, Bahia, Brazil.
Custead M. 2007. Geographic Information Systems: it's role in marine conservation veterinary medicine, ASTER Coreal Reef Classification in Bahia, Brazil, 2002. Universidade Federal da Bahia Escola de Medicina Veterinária, Bahia, Brazil.
Custead M. 2006. *Incidence and prevalence of hemoparasites in wild-caught Australian turtles.* The National Aquarium, Baltimore. Scientific Continuing Education Seminar, Baltimore, MD.
Custead M. 2006. *Incidence and prevalence of hemoparasites in wild-caught Australian turtles*. The National Aquarium, Baltimore. Senior Thesis Presentation. St. Mary's College of Maryland, St. Mary's, MD.

Licensure

New Jersey, 2010 – 2011
District of Columbia, 2011 – 2013
Virginia, 2011 – 2012

Popular Press

Custead M and Palmer K. The Purpose of Blood Transfusion, January 1, 2011. Online.

Continuing Education

Bone Marrow Workshop, West Lafayette, IN, 2014
American Association of Cancer Research, Frontiers in Cancer Preventative Research, Annual International Conference, Maryland, 2013
Purdue Veterinary Teaching Hospital, Annual Fall Conference: West Lafayette, IN, 2012; 2013
Veterinary Cancer Society, Annual Conference: San Diego, CA, 2010; Albuquerque, NM, 2011
Metropolitan New Jersey Veterinary Medical Association, Tinton Falls, NJ , 2010-2011
Association of Reptile and Amphibian Conference, Baltimore, MD, 2006

PUBLICATION

PUBLICATION

1. Custead M, Childress M, Turek J, An R, Nolte D. *Application of Biodynamic Imaging for Personalized Chemotherapy in Canine Lymphoma: A Pilot Study*. 2015. Convergent Science Physical Oncology, in preparation.